IEEE Access
Multidisciplinary | Rapid Review | Open Access Journal

Received October 9, 2019, accepted October 25, 2019, date of publication October 30, 2019, date of current version November 12, 2019.

Digital Object Identifier 10.1109/ACCESS.2019.2950599

Multicore Fiber Scenarios Supporting Power Over Fiber in Radio Over Fiber Systems

CARMEN VÁZQUEZ, (Senior Member, IEEE), JUAN DAYRON LÓPEZ-CARDONA, PEDRO CONTRERAS LALLANA, DAVID SÁNCHEZ MONTERO, FAHAD MOHAMMED ABDULHUSSEIN AL-ZUBAIDI, SANDRA PÉREZ-PRIETO, AND ISABEL PÉREZ GARCILÓPEZ

Electronics Technology Department, Universidad Carlos III de Madrid, 28911 Leganés, Spain

Corresponding author: Carmen Vázquez (cvazquez@ing.uc3m.es)

This work was supported in part by the Spanish Ministry of Science, Innovation and Universities, Directorate for Research and Innovation at Madrid region, and H2020 European Union programme under Grant RTI2018-094669-B-C32 and Grant Y2018/EMT-4892, and in part by FSE and 5G PPP Bluespace project Grant 762055.

ABSTRACT We propose the integration of power over fiber in the next generation 5G radio access network front-haul solutions based on spatial division multiplexing with multicore fibers. The different architectures in both shared- and dedicated- core scenarios for power over fiber delivery and data signals are described. The maximum power to be delivered depending on the efficiencies of the different components is addressed as well as the limits of the delivered energy to avoid fiber fuse and non-linear effects. It is shown how those limits depend on high power laser linewidth, fiber attenuation, link length and fiber core effective area. The impairments related to non-linear effects, multicore fiber crosstalk and temperature are also theoretically analyzed. Experiments show there is no degradation of signal quality for feeding powers of several hundreds of milliwatts for both scenarios in 4-core multicore fibers. This study helps in designing future power by light delivery solutions in Radio over Fiber systems with multicore fibers.

INDEX TERMS Multicore fibers, power by light, optical transmitters, optical receivers, spatial division multiplexing, 5G mobile communications, optical fibers, power lasers, photovoltaic converters, front-haul.

I. INTRODUCTION

The first work proving the concept of using optical fiber to deliver power date back to 1978 [1] in the telecommunications industry to optically power a sound alerter thus demonstrating the feasibility of converting optical power into sound power with good efficiency. Even some analysis of the constraints on optical powering in fiber-in-the-loop are found in 1993 [2]. By that time, in 1996, Power over Fiber (PoF) was proposed to partially power remote antenna sites [3] at tenths of meters, making a special mention to the advantage of the optical fibers' low weight. Since then, the good affinity between PoF and Radio over Fiber (RoF) technology is shown in different experiments using standard multimode silica fibers (MMF) [4], [5]. For feeding with higher optical powers, special double cladding fibers (DCF) as those used in fiber lasers are proposed [6].

The associate editor coordinating the review of this manuscript and approving it for publication was Young Jin Chun.

The upcoming 5G technology opens up new application niches for the PoF technology [7]. The reduction of the cell sizes for providing high bandwidth coverage in RoF communications foresees a huge increment in the power consumption demand by the massive installation of remote radio heads (RRHs). Therefore, low power simplified antenna units are required [8] together with some strategy for energy saving to reduce the impact of the power consumption of the antennas, including the capability of turning into sleep mode some RRHs [9].

The use of multicore fibers (MCF) provides compact designs to develop optical front-haul technologies targeting spatial division multiplexing (SDM) with increased aggregated capacity [10]. MCF can also contribute to downsizing the footprint by using optical fiber composite low-voltage cables. RoF mixed with PoF through MCF can be suitable for small cell operations in advanced radio access networks (RAN) [11], and Centralized RAN performing signal processing at the central office with low power simplified

RRHs [9]. The PoF pooling concept in 5G front-haul architectures with Software Defined Network (SDN) capabilities also uses MCF [12]. Some results in 4-core MCF with simultaneous data and energy delivery with no BER penalty are reported in [13]. Apart from this, most works use each core either for energy or for data delivery with a lack of a systematic analysis of how to optimize the efficiency of a PoF solution along with an estimation of the power limits. Previous PoF systems reported elsewhere focus on successfully feeding the remote node, but no analysis on the PoF performance limitations and optimization issues are addressed.

In this paper, we propose and analyze the integration of the PoF technique in next generation radio access network front-haul architectures with MCF-based deployments. Firstly, a summary of the main parameters of some of the different PoF experiments on RoF systems and of the available PoF commercial products is provided. In section III, dedicated and shared- core scenarios for remote power delivery with added functionalities are described. Next, the energy efficiency delivery is analyzed. It is shown how the limits on the maximum power to be distributed depend on laser linewidth, fiber attenuation, link length and fiber core effective area. In addition, impairments due to non-linear effects and crosstalk issues in MCFs are described and discussed. For the analysis, section IV describes the mathematical framework to firstly delimit the dominant effects meanwhile the resulting values are the starting point in section V to get more precise results. Within this section, simulation results using Virtual Photonics Instrumentation (VPI) tool and some experimental results are also provided confirming the expected behavior. Finally, section VI is devoted to the conclusions.

II. STATE OF THE ART OF POWER OVER FIBER ON ROF SYSTEMS

In the following, a summary of the main achievements in PoF applied to RoF and commercial products are reported.

In the first experiments [3], the optical powered parts at the antenna site included the local oscillator and its driver, demanding up to 4 W of electrical power. For this purpose, 8 fibers (200 μm core diameter) were deployed in parallel to perform analog beam forming at a distance of tens of meters. In [14], a High Power Laser (HPL) at 1480 nm and photovoltaic converters (PVC) provided 26.5 mW at 2 km, multiplexing power and data, with RoF transmission at the 2.4 GHz band. In 2008, it was proposed feeding in-building antenna units [5], using 2 W at the Central Office (CO) to optically power 8 antennas at the RRH site located at 300 m, providing electrical powers of 100 mW, through MMFs and employing 850 nm HPLs. In [15], the distance was increased up to 500 m by using 3 modules capable of providing an electrical power of 300 mW each, in a RoF link at 19.2 GHz. In 2008, it was further demonstrated the possibility of multiplexing power and data into the same MMF fiber lead for RoF applications with negligible signal penalties. It was used a 834 nm HPL with data signal transmitted at 1300 nm, but employing optical feeding powers of 125 mW, well below the 300 mW-handling limit of the multiplexer (MUX) device used at the input [16].

In 2012, in an energy-autonomous pico-cell scenario for home applications, a PoF topology using coarse wavelength division multiplexing but using a HPL at 980 nm was reported [17], providing lower levels of electrical power (60 mW) at 100 m through MMF fibers. The multiservice concept by integrating 10 GbE traffic (10 Gigabit Ethernet), RoF signal transmission (IEEE 802.11g modulation scheme) and PoF into the same fiber lead was developed.

Higher feeding powers from the CO were reported in [18], with a 105 μm cladding diameter DCF fiber for power delivery and optical feeding powers of 60 W at 808 nm, but limited to 300 m. There were no PVCs at the remote site, where 26 W were measured with a power meter (PM). Later, RoF transmission at 1300 nm (64 QAM carrier at 2.4 GHz and bit rate of 54 Mbps) with a 10 W PoF feeding system at CO using a conventional MMF was further demonstrated. The link length was extended up to 4 km by using a 1550 nm HPL [19] but without PVCs, claiming 6 W of optical power at the remote site. Most recently, 150 W PoF feeding with RoF transmission using a 1 km-long DCF link [6] has been reported.

In terms of long distance demonstrations, an optically powered switch to interrogate a sensor network at 100 km [20] was also proposed. Although in the context of radio access networks, link lengths are up to 20 km.

More recently, optically powered systems based on novel MCFs have been proposed. A 100 GHz Uni-Traveling Carrier Photodiode (UTC-PD), and a low-power-consumption RF amplifier were optically powered through 4 dedicated cores in a 7-core MCF [8] providing electrical powers of 80 mW. The wavelength of the HPL PoF source was 1550 nm. In [11] the gate of an improved UTC-PD was optically powered with 50 mW of electrical power using 4 dedicated cores from a 7-core MCF in experiments with 1 m wireless coverage and employing a 92 GHz RoF carrier. However there was no specific information about the MCF link length. MCF was also proposed in the PoF pooling concept in 5G frounthaul architectures with SDN [12] and more recently in SDN/NFV front-haul networks deploying simultaneously Analog RoF (ARoF) and PoF [21]. Experiments in a 20 m-long 4-MCF link with simultaneous data (2.6 Gbps) and energy delivery (320 mW/core) show no BER penalty [13].

A summary of the main parameters of some of the different PoF experiments on RoF systems previously described is shown in Table 1. In terms of commercial products available there is no a specifically oriented off-the-shelf solution for RoF systems neither using MCF for the remote power distribution. They are mainly offered in a general-purpose configuration using standard MMF, with core diameters of either 62.5 or 100 μm, and operating wavelengths of 830 nm [22], 976 nm [23] or both [24]. Delivered powers ranging from 0.25 W to 1 W at different link lengths, usually below 1 km, are only available.

TABLE 1. PoF experiments on RoF systems.

Power at CO (optical)	Power at remote site (electrical)	Powered devices	Test distance (m), Fiber type core (μm)	HPL (nm)	Source/ year
8x1 W/ch	8x 0.5 W/ch	8 antennas, analog beam forming	12.2, MMF:200	750-850	[3] 1996
0.3 W	26.5 mW	UTC-PD+low power amplifier	2000 data/power	1480	[14] 2005
2 W	100 mW	8 antennas. PA+LO	300, MMF: 50	850	[5] 2008
1 W/RRH	60 mW/RRH	RRH (LD +PD+amplifier)	100, MMF: 50	980	[17] 2012
60 W	Optical: 26 W	PM, no PVC	300, DCF:105	808	[18] 2015
10 W	Optical:6 W	PM, no PVC	4000, MMF: 62.5	1550	[19] 2018
150 W	7 W	PVCs silicon based	1000, DCF : 125	808	[6] 2019
0.1 W	21 mW/ core, 80 mW total	UTC-PD + RF PA	MCF-7 cores	1550	[9] 2016
0.2 W (x4)	50 mW total	UTC-PD + RF PA	MCF-7 cores	1549.3	[11] 2018
0.32 W/core	Optical: 70 mW	PM, no PVC	20+100, MCF-4+SMF	1480	[13] 2019

Note: MCF experiments in shadow grey. LO=Local Oscilator. PA=Power Amplifier.PM=Power Meter. UTC-PD=Uni-Traveling Carrier Photodiode. LD=Laser Diode

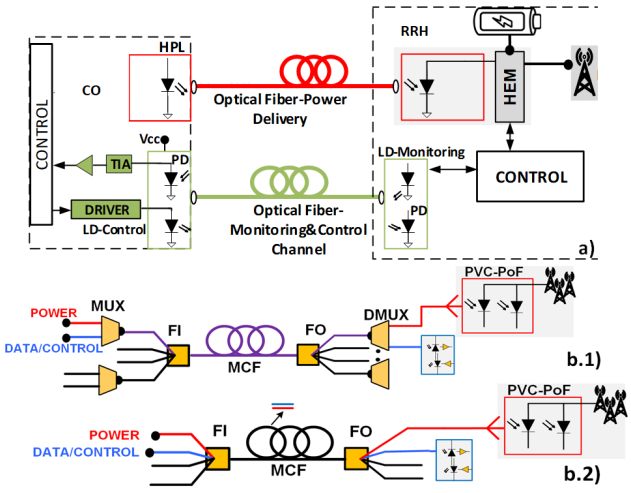

FIGURE 1. (a) PoF system with power and control channels. (b) Powering architectures. (1) shared cores: power and data/control multiplexed on the same core. (2) dedicated power cores. PVC = Photovoltaic converter, FI: Fan-In device, FO: Fan-Out device, MCF: Multicore fiber.

III. POWERING ARCHITECTURES

There are novel front-haul technologies in support of the RAN growing traffic demand based on the introduction of SDM to increase the aggregated capacity of the infrastructure [10]. SDM can be achieved either using bundles of fibers or more compact designs based on MCFs. Some MCF in field test-beds are currently under development [25]. In this framework, a PoF system for delivering power to a generic RRH at the remote site, with both power and control channels, is shown in Fig.1.a. In the power over MCF transmission, there are two main scenarios [13]:

- "shared cores", some individual cores of a MCF transmit simultaneously the data/control and PoF signals,
- "dedicated power cores", one or more of the individual cores of a MCF are only used for optically feeding the RRH.

Fig.1.b1 and Fig.1.b2 show these proposed powering architectures. Fan-in (FI) devices feed power to each core whereas Fan-out (FO) devices spatially separate the signals coming from each core. CO and RRH include additional MUX/DMUX devices in a shared core scenario. Meanwhile, the PoF signal is directly launched into an individual core in the dedicated scenario with no data/control traffic. All these passive devices should at the same time handle high optical powers, have small insertion losses and provide high crosstalk. Adding a bandpass filter at the data/control central channel wavelength increases the isolation. Apart from the remote optical power supply capability other functionalities may be included such as a rechargeable battery to keep an energy source to support energy efficiency techniques [9] based on tuning the RRH into sleep mode to reduce the power demand. This battery can also be used to backup operations and to provide feedback to the CO in case of failure. The remote node gives information of the RRH to the CO. A Hardware Energy Manager (HEM) supports those capabilities. PoF integration in existing infrastructures is feasible but requires high power passive devices, HPLs and PVCs; being affordable in a centralized configuration thus sharing the cost between multiple users and with successful energy efficiency strategies for reducing the overall power consumption.

IV. ENERGY EFFICIENCY AND TRANSMISSION MEDIA

The overall efficiency of the system is a critical design factor in any PoF system. It directly depends on: the electrical-to-optical conversion efficiency at the transmitter site, *N1*, the transmission efficiency of the optical distribution network, *N*2, and the optical-to-electrical conversion efficiency of the photovoltaic converter, *N3*, at the remote node. Previous studies [7], [26] define the product of *N2* and *N*3 as the System Energy Efficiency (SEE). In this work, we expand this figure of merit by adding the *N*1 term, which includes the coupling efficiency between the HPL and the optical fiber. Losses due to connectors are considered in either *N1, N2* or *N3* depending on their placement. The Global Energy Efficiency (GEE) in a PoF system is given then by

$$GEE = \frac{\text{Energy provided to Load at RRH}}{\text{Energy provided to HPL}} = N1\,N2\,N3 \quad (1)$$

N2, depends of the type of optical fiber used for power delivery. PoF systems use specialty fibers such as DCFs or standard counterparts either single mode (SMF), MMF or MCF, see Table 1.

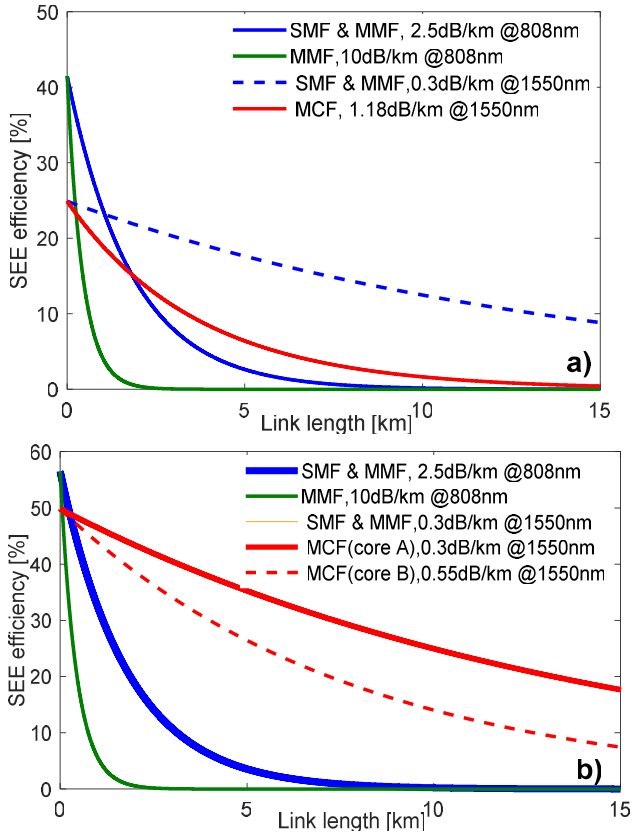

FIGURE 2. PoF system energy efficiency, SEE, vs link length for different wavelengths. 100% HPL-fiber coupling efficiency. PVC efficiency and optical fiber loss: (a) commercial devices; (b) state of the art devices.

The optical fiber selection for the power distribution network determines the efficiency of the system versus distance and the power that can be delivered to the remote site. This power depends on the transmission loss, the optical fiber damage threshold and the non-linear effects. All those aspects are analyzed next, in a systematic way following the approach for optical fiber lasers from [27].

A. OPTICAL POWER LOSSES

The transmission loss increases exponentially with the link length, L. It depends on the operating wavelength that determines the optical fiber attenuation as well as the conversion efficiency of the PVC. We consider different optical fibers and operating wavelengths: commercial PVC conversion efficiencies and optical fibers [28], [29]; expected PVC conversion efficiencies and MCF in literature [30]. The SEE is calculated for a HPL at 808 nm and silica MMF fibers with core diameters of 200 μm, and 62.5 μm (G.651); and a HPL at 1550 nm with standard SMF and MCF fibers.

The analysis considers different link lengths up to 15 km in a mobile front-haul convergent with Passive Optical Networks [10]. For MMF G.651, see Fig. 2.a, with current commercial PVCs, there is a better efficiency for a HPL operating at 808 nm for link lengths shorter than 1.1 km and up to 2 km for commercial MCF [28] with 1.1 dB/km loss. For the 200 μm MMF, only for link lengths shorter than 270 m the efficiency is better at 808 nm. If the power requirements are higher or the coupling loss factor ($N1$) decreases, the 200 μm MMF with HPL at 808 nm has a better performance even for longer distances.

In the near future, with improved PVC conversion efficiencies, it is always more efficient to work at longer wavelengths if there is no restriction on power limits. For MCFs with low losses [30], they show similar results to SMF. However, a different SEE performance for each core suffices, see Fig. 2.b, because of the asymmetry between the different cores in a MCF. The different attenuation coefficient between the central and external cores, core A and core B curves in Fig. 2.b, implies reducing the distances in around 100 m to achieve the same performance.

B. INPUT POWER LIMITS

In this study we consider the ultimate fiber damage power density threshold, I_{th}, to be 2.5 MW/cm^2 [31]. This value strongly depends on the mode field diameter (MFD) that determines the fiber effective mode area (A_{eff}).

The analysis of the fiber effective area of the fundamental mode provides an upper bound condition to the threshold power injected into the fiber to avoid fiber damage, even in the case of MMF, and assuming a Gaussian power distribution launched into the fiber. Thus, the maximum damage threshold power, P_{th}, is given by:

$$P_{th} = I_{th} \cdot A_{eff} \tag{2}$$

As a first approximation we estimate the MFD and the effective diameter, d_{eff}, as in [32]; being the effective area:

$$A_{eff} = \pi \cdot \left(\frac{d_{eff}}{2}\right)^2 \tag{3}$$

Regarding the non-linear effects, the threshold power of both Stimulating Brillouin Scattering (SBS) and Stimulating Raman Scattering (SRS) are given by [33]:

$$P_{SBS} = \frac{21 \cdot k \cdot A_{eff}}{g_B \cdot L_{eff}} \cdot \frac{\Delta\nu_B + \Delta\nu_P}{\Delta\nu_B} \tag{4}$$

Being g_B the Brillouin gain coefficient, around $6 \times 10^{-11} m/W$ for silica $k = 2$ random polarized HPL, $\Delta\nu_B$ the Brillouin gain bandwidth (35 MHz), and $\Delta\nu_p$ the pump laser linewidth, whereas:

$$P_{SRS} = \frac{16 \cdot A_{eff}}{g_R \cdot L_{eff}} \tag{5}$$

where g_R stands for the Raman gain coefficient, around $1 \times 10^{-13} m/W$ (1/2 for non-polarized light) for silica.

In both cases L_{eff} is the effective fiber length that depends on L and fiber attenuation coefficient, α as follows:

$$L_{eff} = \frac{1 - e^{-\alpha \cdot L}}{\alpha} \tag{6}$$

We analyze step index fibers and take into account the fiber fuse phenomenon and the non-linear effects as boundary

limits as in [27]. The A_{eff} is calculated first, considering d_{eff} as the physical diameter of the fiber core, d. As we increase the input power, we estimate which non-linear effect either SBS or SRS appears first and then we compare the selected one with the maximum threshold power for fiber fuse. SBS power threshold increases linearly with $\Delta\nu_p$, see (4), so a broad HPL linewidth reduces this effect. P_{SRS} and P_{SBS} have the same dependence on A_{eff} and L_{eff}. It can be seen that:

$$\frac{P_{SRS}}{P_{SBS}} = \frac{16g_B}{21kg_R}\frac{\Delta\nu_B}{\Delta\nu_B + \Delta\nu_P} \tag{7}$$

P_{SRS} dominates over P_{SBS} for HPL linewidths ($\Delta\nu_p$) > 8 GHz.

Fig. 3 shows the optical power limits versus link length (from 200 m to 20 km, 100 m step), fiber core diameter (from 4 to 80 μm, 1 μm step), HPL linewidth (2 GHz and 8 GHz), being $\Delta\nu_p = \Delta\nu_{HPL}$, and optical fiber attenuation coefficients (0.2 dB/km and 1 dB/km). The discontinuous line shows the link length where the dominant effect changes. There are markers ($*$) on the specific diameters: 6, 8, 9, 50 and 62.5 μm corresponding to some fibers reported on Table 2. The maximum link length for avoiding the non-linear effect influence versus fiber fuse phenomenon depends on both the source linewidth and the fiber losses. For silica fibers, using a 2 GHz to 7 GHz linewidth HPL, this maximum length varies from around 1.8 km (see Fig. 3.a) to 6 km. For an 8 GHz linewidth HPL, this length increases up to 7.8 km (see Fig. 3.b). When non-linear effects are dominant, the slope of the power limit contour plots versus diameter, see Fig. 3.a, shows that to keep the maximum power at 1 W there is a need of greater fiber diameters. On the other hand, this slope decreases when fiber attenuation increases for the same source linewidth. For higher losses, there is no influence of non-linear effects, see Fig. 3.c.

We further analyze in more detail a specific MCF, considering the wavelength dependence of fiber attenuation and A_{eff}. We select a 7-core MCF with low attenuation, 0.3 dB/km [30] and a commercial fiber [28], with 1 dB/km. The d_{eff} is derived for different wavelengths [32] from the manufacturer refractive index profile. It is used the attenuation wavelength dependence of the SMF-28e at short wavelengths (760-900 nm) and the 7-core MCF values [30] for the central and external cores at longer wavelengths (1300-1500 nm).The attenuation of the commercial fiber is only used at 1550 nm. The behavior at 1480 nm is marked with an asterisk in the contour plots of Fig. 4, corresponding to an effective diameter of 5.923 μm. As expected, SRS dominates over SBS for a 8 GHz HPL linewidth, see Fig. 4. The power limit of 500 mW per core at 1480 nm is achieved at 13.7 km. The difference in power limit from central to external cores from 1300 to 1500 nm [30] or effective core diameters from 5.57 to 6.07 μm increases if SRS dominates (see Fig. 5). The fiber fuse is the limiting effect for lengths shorter than 9 or 12 km for the central and external core, respectively.

There is a power limit of 500 mW in central core for link lengths of 13.5 km and this limit increases up to 600 mW

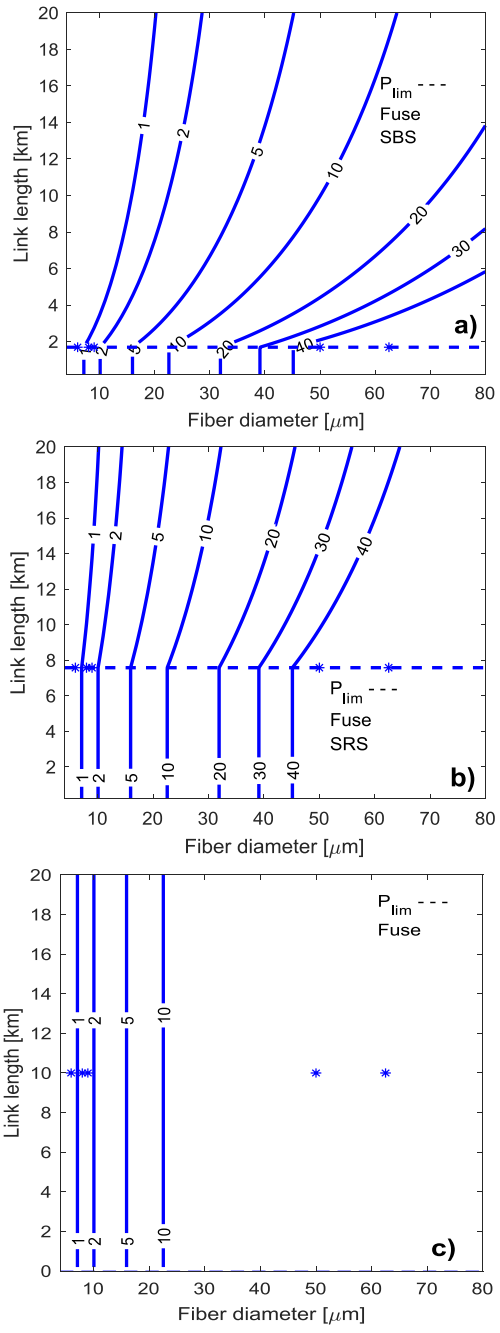

FIGURE 3. Power limit vs fiber diameter and link length. Power units in W. Contour plots of the minimum of the 3 effects (SBS, SRS and fiber fuse). ($*$) 6, 8, 9, 50 & 62.5 μm diameters: (a) α = 0.2dB/Km, $\Delta\nu_{HPL}$ = 2 GHz, (b) α = 0.2dB/Km, $\Delta\nu_{HPL}$ = 8 GHz, (c) α = 1 dB/Km, $\Delta\nu_{HPL}$ = 8 GHz.

in the external core at 15.6 km. By using all cores, 7-core fibers can handle up to 3.5 W meanwhile SMF with the same cladding diameter only handles 1.5 W. At short distances, fiber fuse is the dominant effect with higher powers. In this situation, the power threshold limit has a quadratic response versus the effective core diameter and shows no link length dependency.

In general, as shown in the simulations and in equations (2) to (7) the power over fiber system delivers a maximum optical

TABLE 2. Different fiber types and parameters.

Fiber	4-MCF [28]	7-MCF [28]	7-MCF [34]	19-MCF [34]	7-MCF [35]	MMF
A_{eff} (μm^2)	50.6	28.3	75	85	110	1256

A_{eff}: Effective area per core in MCF

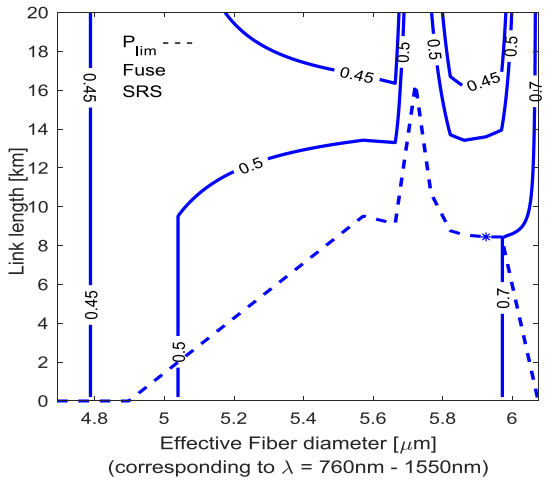

FIGURE 4. Plots of the minimum of 3 physical power limits (SBS, SRS and fiber fused) in a 7-core MCF [30] for different wavelengths and link lengths. Power units in W. Dot point (∗) at 1480 nm. $\Delta\nu_{HPL} = 8$ GHz.

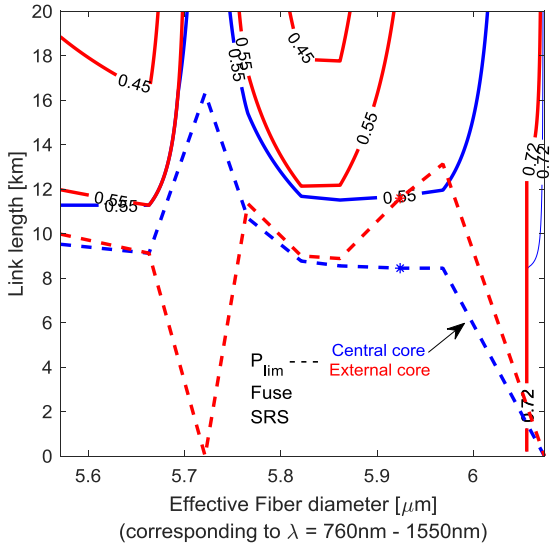

FIGURE 5. Contour plots of the minimum of 3 physical power limits (SBS, SRS and fiber fused) in a 7-core MCF [30] for different wavelengths and link lengths. Power units in W. $\Delta\nu_{HPL} = 8$ GHz Central core (blue) external core (red). Dot point (∗) at 1480 nm.

power proportional to the effective area. This fact implies that for the same cladding diameter, for a weakly-coupled N-MCF, with the same refractive index profile, the higher the number of cores N, the smaller the maximum optical power delivered by each core. Although if all the cores deliver power, the total delivered power increases.

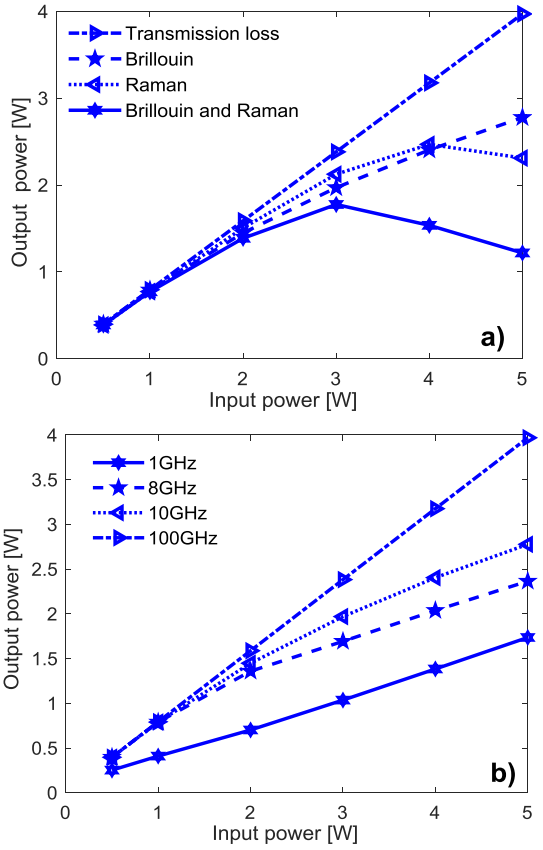

FIGURE 6. Output power vs input power. 1480 nm HPL. 5 km of SMF: (a) 10 GHz linewidth. Attenuation, SBS, SRS independently and all together (b) SBS on & SRS off for different HPL linewidths.

V. IMPAIRMENTS AND EXPERIMENTAL RESULTS

In this section, we identify and discuss some effects that optical power delivery can have on the system performance and how this can affect the efficiency in power delivery.

A. NON-LINEAR EFFECTS ON POWER DISTRIBUTION

This section includes a deeper analysis to check the linewidth required to avoid SBS and to quantify the impact of non-linear effects and attenuation on the power delivery efficiency in both scenarios. We use Virtual Photonics Instrumentation software tool. As we are interested in analyzing the maximum link length considered in front-hauling of tens of km, we consider a HPL at 1480 nm with a 10 GHz linewidth. In these conditions, on silica fibers, as derived in the previous section, SRS dominates for link lengths longer than 8 km with a power threshold of around 1 W at 10 km; we then select 5 km to discuss all possible effects. The output power versus input power for a 5 km link length, with a HPL at 1480 nm and 10 GHz source linewidth is shown in Fig.6.a for a dedicated core scenario. For comparison purposes, we simulate independently transmission loss, SBS and SRS effects and then all together. Up to 1 W input power, only the optical fiber attenuation term decreases the optical power delivery efficiency, SEE. At higher power levels, both SBS and SRS

additionally penalize SEE, in a small amount up to 2 W. The penalties increase up to 75% at 5 W. SBS is fully avoided by increasing the source linewidth. Fig.6.b shows that 100 GHz source linewidths are required. Then HPL such as fiber lasers or multimode laser diodes with typical nm linewidths can be used.

We now simulate dedicated and shared core scenarios for 7-core MCF. In both cases, a filter centered at the data channel wavelength is placed at the output. The 7-core MCF is modelled with a new Raman gain curve for silica fibers with an effective area of 27 μm^2 as a first approximation. The input data channels are in the C band. Output power versus input power up to 2 W, for both scenarios, is shown in Fig.7.a and 7.b. In both scenarios, the power over 7-core MCF transmission is not penalized by non-linear effects up to 1 km for 2 W input power in each core. Meanwhile for 5 km, the power over 7-core MCF transmission for the same 2 W input power is dramatically penalized in the shared core scenario, with only 10% optical power reaching the PVC versus 90% in the dedicated core scenario. In power over 7-core MCF using all cores for power delivery in a dedicated scenario, 4.9 W input power is delivered up to 10 km (1 W/core is the limit for non-linear effects and around 0.7 W/core for fiber fuse), with SEE limited only by loss penalty. In the shared core scenario, SRS degrades even more the SEE limiting the power to 0.4 W/core, being the maximum delivered power of 2.8 W in total. This value is still higher than those shown in Fig.3 in SMF. In general, SEE decreases at a greater extent in the shared core scenario, but in a dedicated scenario there is less cores for data transmission. Simulations including the higher core doping in MCF should provide stronger Raman effects.

B. CROSSTALK

The MCF crosstalk (XT) makes that a specific core delivers a different signal than initially considered. In a dedicated scenario, where all cores only propagate energy there is no effect for power levels far away from the limits discussed on previous sections. In a dedicated scenario, with some cores delivering energy and others data, and in a shared core scenario, those undesired signals could affect the transmission quality. Considering PoF signals of few W for power delivery and data signals of several mW or lower, the undesired signal can also saturate the photodetector. An optical filter, centered at the data channel wavelength, filters the undesired signal from the other core at 1480 nm. This filter provides isolation to crosstalk from MCF fan-out devices but the leakage of this energy reduces the PoF SEE. If the undesired signal from the other core is part of SRS of HPL centered at C band, the filter is neither a solution.

As a first conservative approximation, to assure no negative impact in data transmission we consider good designs those with power over MCF at least one order of magnitude lower than data signals, or a XT greater than −40 dB for all link lengths. The XT between two cores in a MCF depends on power transfer efficiency, η, and is given by [36]:

TABLE 3. 7-Core MCF fiber structural parameters.

	Fiber B [33]	Fiber A [26]
Core diameter (μm)	5.3	5.5
Core separation (μm)	35.4	35
Cladding diameter (μm)	125.9	125
Relative refractive index difference, Δ	0.7%	1.017%

$$XT(z) = \frac{1 - e^{-2\cdot\frac{\eta}{L_c}\cdot z}}{1 + e^{-2\cdot\frac{\eta}{L_c}\cdot z}} \tag{8}$$

$$\eta = \sin^2\left(\frac{\pi \cdot z}{2 \cdot L_c}\right) = \sin^2(k \cdot z) \tag{9}$$

where $L_c = \pi/(2\cdot k)$ is the coupling length with k the coupling coefficient; z the propagation distance along the fiber axis.

We calculate the effective refractive index difference of MCF with a software tool based on the Finite Element Method with a full vectorial implementation, a mode solver named FemSIM. We compare two 7-core MCF with the parameters reported in Table 3. The XT for both fibers at 1550 nm worsens with the link length, see Fig. 8 being better than −50 dB up to 10 km for Fiber A. They are in accordance with the values provided in [36]. We also analyze the influence of temperature (T) on XT in case that the power over MCF transmission induces T increments. The refractive index of the core of a silica fiber versus temperature is expressed as:

$$n_{\text{core}}(T) = n_{\text{core}}(T = 0K) + \frac{dn}{dT} \cdot T[K] \tag{10}$$

The slope can have different values ranging from 7.0978×10^{-6} [37] to 11.8×10^{-6} [38]. The 7-core MCF Fiber A has a core refractive index of 1.475 at 298 K, and we consider previous silica variation range to obtain the following equation:

$$n_{\text{core}}(T) = (1.4722\pm0.0007)+[(9.44910^{-6})\pm(2.35110^{-6})]T \tag{11}$$

The core refractive index average value and the maximum positive and negative deviation at a specific temperature are used in the simulations. The effective refractive indexes are calculated again using FemSIM for a specific set of temperatures and then extrapolated for the whole range. The XT variation with link length for different temperatures using (11) is calculated, and XT changes in a 10 °C-span variation are negligible. When considering the temperature effect on XT for a specific link length, there is almost a constant slope of 0.136 dB/°C. When the temperature increases, the core refractive index increases as well and a better crosstalk is expected meanwhile a reduction in the temperature worsens the XT performance.

Some measurements are reported in next section confirming that this XT analysis assures no penalty in either dedicated or shared core scenarios.

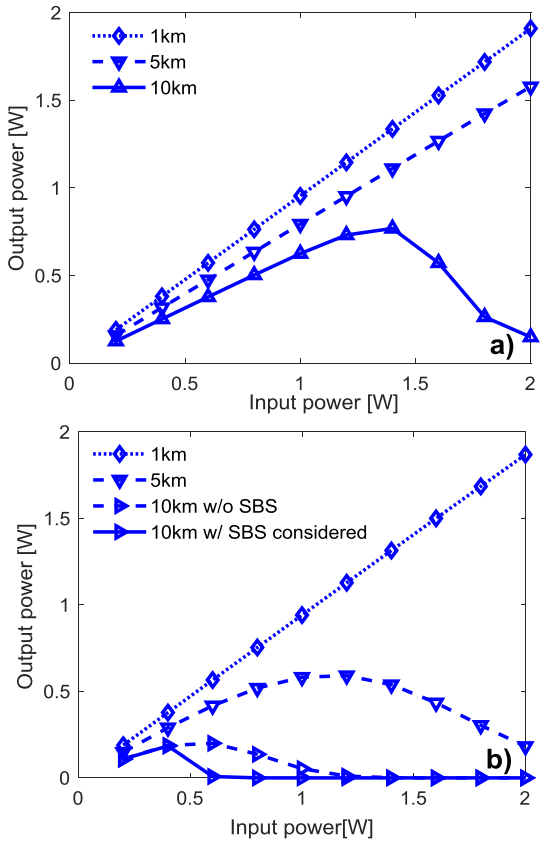

FIGURE 7. Output power vs input power. 1480 nm HPL, 100 GHz linewidth. 7-core MCF: (a) dedicated scenario, (b) shared scenario with C-band channels.

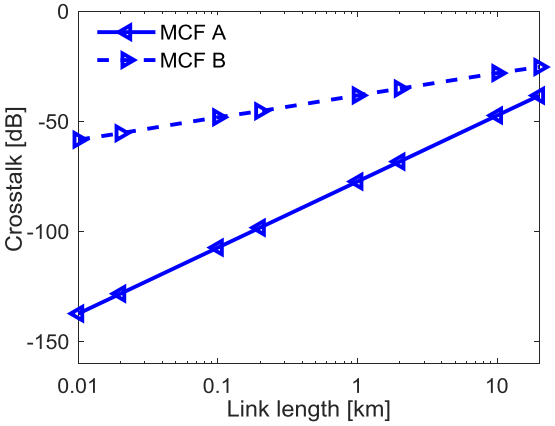

FIGURE 8. Crosstalk vs link length for different 7-core MCF fibers: A and B (see Table 3).

C. EXPERIMENTAL RESULTS

A BER tester using a SFP transceiver operating at 1550 nm is used to generate and evaluate the BER performance of a 2.6 Gbps bit-rate data traffic signal (NZR, PRBS $= 2^{31}-1$). PoF is provided by a fiber HPL at 1480 nm with 2 nm linewidth to avoid SBS. The set-up is described in [10], but a MCF link of 200 m is used. The MCF is a single mode 4-core MCF with MFD of 7.5-8.4 μm [28], so according to

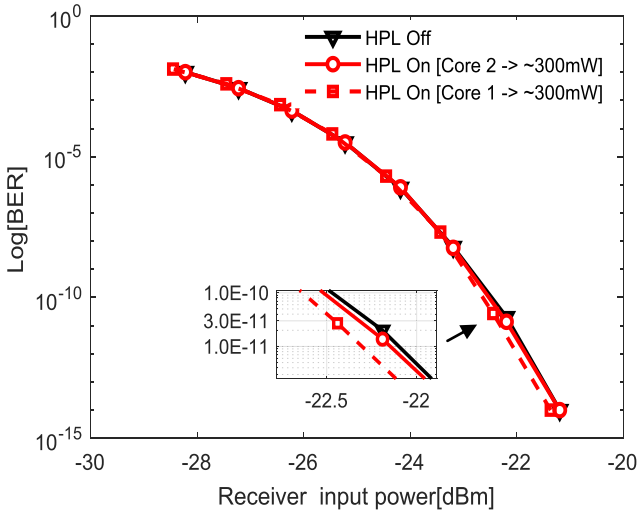

FIGURE 9. BER impact results in both scenarios: dedicated (HPL on core 2) and shared (HPL and data on core 1). Feeding 300 mW optical power PoF signal per core.

Fig. 3 supporting up to 1 W/core. In both cases, the PoF feeding power into the MCF fan-in device is fixed to 300 mW, limited by FI power-handling device requirements. BER measurements for the dedicated and shared core scenarios are shown in Fig. 9 showing the negligible impact of PoF on the data transmission quality. Measured BER values are better than 10^{-11} with power over MCF delivering 100 mW at remote node. The measured XT is better than -50 dB.

VPI simulations are also performed in a 5 km link, showing no BER degradation in any of the proposed scenarios.

VI. CONCLUSION

We introduced the dedicated and shared core scenarios in power over MCF fibers for integration of PoF in next-generation radio access networks based on MCF for low power consumption RRH. Simulations of the limitations on maximum power and energy delivery efficiency in both scenarios and with other types of fibers are provided. The maximum feeding power per core is proportional to MFD and the power over MCF efficiency decreases for longer link lengths, mainly due to SRS when using HPL linewidths greater than 100 GHz. The higher net effective area using all cores in MCF improves the power delivery efficiency in comparison to SMF. In weakly-coupled 7-core MCF, in both scenarios, power over MCF is not penalized by non-linear effects up to 1 km for 2 W input power in each core. Meanwhile for 5 km, in the shared core scenario only 10% optical power reaches the RRH versus 90% in the dedicated core scenario. In the dedicated scenario using all cores for power over MCF, neither crosstalk nor a reduced SRS penalty is expected. In the dedicated scenario using only some cores and in the shared core scenario, more restrictions on power over MCF apply to avoid degradation of signal quality. The shared core scenario has higher losses and additional components are required, but resources are shared between power

over MCF and data transmission. Depending on the MCF parameters, there is a maximum link length to avoid any effect from crosstalk and temperature effects. Measurements show no BER degradation of signal quality for feeding PoF power of 300 mW in 4-core MCF in any of the proposed scenarios.

ACKNOWLEDGMENT

The support of Arantzazu Nuñez is acknowledged.

REFERENCES

[1] B. C. DeLoach, R. C. Miller, and S. Kaufman, "Sound alerter powered over an optical fiber," *Bell Syst. Tech. J.*, vol. 57, no. 9, pp. 3309–3316, Nov. 1978.

[2] T. C. Banwell, R. C. Estes, L. A. Reith, P. W. Shumate, and E. M. Vogel, "Powering the fiber loop optically—A cost analysis," *J. Lightw. Technol.*, vol. 11, no. 3, pp. 481–494, Mar. 1993.

[3] A. P. Goutzoulis, J. M. Zomp, and A. H. Johnson, "Development and antenna range demonstration of an eight-element optically powered directly modulated receive UHF fiberoptic manifold," *J. Lightw. Technol.*, vol. 14, no. 11, pp. 2499–2505, Nov. 1996.

[4] D. Wake, A. Nkansah, and N. Gomes, "Optical powering of remote units for radio over fiber links," in *Proc. Int. Topical Meeting Microw. Photon. (MPW)*, Victoria, BC, Canada, 2007, pp. 29–32.

[5] D. Wake, A. Nkansah, N. J. Gomes, C. Lethien, C. Sion, and J. P. Vilcot, "Optically powered remote units for radio-over-fiber systems," *J. Lightw. Technol.*, vol. 26, no. 15, pp. 2484–2491, Aug. 2008.

[6] N. Tajima, D. Kamiyama, and M. Matsuura, "150-watt power-over-fiber feed for bidirectional radio-over-fiber systems using a double-clad fiber," in *Proc. Opt. Fiber Commun. Conf. Exhib. (OFC)*, San Diego, CA, USA, 2019, pp. 1–3, Paper W1I.7.

[7] C. Vázquez, D. S. Montero, P. J. Pinzón, J. D. López-Cardona, P. Contreras, and A. Tapetado, "Integration of power over fiber on RoF systems in different scenarios," *Proc. SPIE*, vol. 10128, Jan. 2017, Art. no. 101280E.

[8] T. Umezawa, A. Kanno, P. T. Dat, K. Akahane, Y. Awaji, N. Yamamoto, and T. Kawanishi, "Multi-core based 94-GHz radio and power over fiber transmission using 100-GHz analog photoreceiver," in *Proc. 42nd Eur. Conf. Opt. Commun. (ECOC)*, Dusseldorf, Germany, 2016, pp. 1–3.

[9] J. Zuo, J. Zhang, C. Yuen, W. Jiang, and W. Luo, "Energy efficient user association for cloud radio access networks," *IEEE Access*, vol. 4, pp. 2429–2438, 2016.

[10] J. M. Galve, I. Gasulla, S. Sales, and J. Capmany, "Reconfigurable Radio access networks using multicore fibers," *J. Quantum Electron.*, vol. 52, no. 1, Jan. 2016, Art. no. 0600507.

[11] T. Umezawa, P. T. Dat, K. Kashima, A. Kanno, N. Yamamoto, and T. Kawanishi, "100-GHz radio and power over fiber transmission through multicore fiber using optical-to-radio converter," *J. Lightw. Technol.*, vol. 36, no. 2, pp. 617–623, Jan. 15, 2018.

[12] G. Otero, J. D. López-Cardona, R. Muñoz, C. Vázquez, D. Larrabeiti, R. Vilalta, J. A. Hernández, and J. M. Fábrega, "SDN-based multi-core power-over-fiber (PoF) system for 5G fronthaul: Towards PoF pooling," in *Proc. 44th Eur. Conf. Opt. Commun. (ECOC)*, Rome, Italy, Sep. 2018, pp. 1–3.

[13] C. Vázquez, D. S. Montero, F. M. A. Al-Zubaidi, and J. López-Cardona, "Experiments on shared- and dedicated- power over fiber scenarios in multi-core fibers," in *Proc. 28th Eur. Conf. Netw. Commun. (EuCNC)*, Jun. 2019, pp. 412–415.

[14] N. Nakajima, "RoF technologies applied for cellular and wireless systems," in *Proc. Int. Top. Meeting Microw. Photon.*, Seoul, South Korea, Oct. 2005, pp. 11–14.

[15] D. H. Thomas, G. V. de Faria, and J. P. von der Weid, "Fully powered-over-fibre remote antenna unit," in *Proc. Int. Top. Meeting Microw. Photon. Jointly Held Asia–Pacific Microw. Photon. Conf.*, Gold Coast, QLD, Australia, Sep./Oct. 2008, pp. 102–105.

[16] D. Wake, N. J. Gomes, C. Lethien, C. Sion, and J.-P. Vilcot, "An optically powered radio over fiber remote unit using wavelength division multiplexing," in *Proc. Int. Top. Meeting Microw. Photon. Jointly Held Asia–Pacific Microw. Photon. Conf.*, Sep./Oct. 2008, pp. 197–200.

[17] C. Lethien, D. Wake, B. Verbeke, J.-P. Vilcot, C. Loyez, M. Zegaoui, N. Gomes, N. Rolland, and P.-A. Rolland, "Energy-autonomous picocell remote antenna unit for radio-over-fiber system using the multiservices concept," *IEEE Photon. Technol. Lett.*, vol. 24, no. 8, pp. 649–651, Apr. 15, 2012.

[18] M. Matsuura, H. Furugori, and J. Sato, "60 W power-over-fiber feed using double-clad fibers for radio-over-fiber systems with optically powered remote antenna units," *Opt. Lett.*, vol. 40, no. 23, pp. 5598–5601, 2015.

[19] H. Kuboki and M. Matsuura, "Optically powered radio-over-fiber system based on center- and offset-launching techniques using a conventional multimode fiber," *Opt. Lett.*, vol. 43, no. 5, pp. 1067–1070, 2018.

[20] M. Bravo, M. A. Erro, J. M. Algueta, S. Diaz, and M. Lopez-Amo, "Remote fiber optic switch powered by light for robust interrogation of fiber Bragg grating sensor networks," *Meas. Sci. Technol.*, vol. 24, no. 9, 2013, Art. no. 094021.

[21] R. Muñoz, R. Vilalta, C. Manso, L. Rodríguez, J. M. Fábrega, R. Martínez, R. Casellas, J. Brenes, G. Landi, M. Capitani, G. Otero, D. Larrabeiti, C. Vázquez, J. D. López-Cardona, E. Grivas, T. Lagkas, D. Klonidis, S. Rommel, and I. T. Monroy, "Experimental demonstration of advanced service management in SDN/NFV front-haul networks deploying ARoF and PoF," in *Proc. Eur. Conf. Opt. Commun. (ECOC)*, Dublin, Republic of Ireland, 2019, pp. 459–463.

[22] RLH Industries. *Power Over Fiber System (PoF)*. [Online]. Available: https://www.fiberopticlink.com/product/power-over-fiber-system-pof/#tab-id-5

[23] *MH GoPower*. Accessed: Dec. 10, 2018. [Online]. Available: http://www.mhgopower.com/laser_pof_concept.html

[24] JDSU. *JDSU Power Over Fiber Module*. Accessed: Dec. 10, 2018. [Online]. Available: http://www.laser-technology.com/component/k2/item/193-power_over_fibre

[25] C. Antonelli, D. Cassioli, F. Franchi, F. Graziosi, A. Marotta, M. Pratesi, C. Rinaldi, and F. Santucci, "The city of L'Aquila as a living lab: The INCIPICT project and the 5G trial," in *Proc. IEEE 5G World Forum (5GWF)*, Jul. 2018, pp. 410–415.

[26] Y. Bi, S. Shen, J. Jin, K. Wang, and L. G. Kazovsky, "Remotely powered and reconfigured quasi-passive reconfigurable nodes for optical access networks," *J. Electr. Comput. Eng.*, vol. 2016, Jan. 2016, Art. no. 2938415.

[27] J. W. Dawson, M. J. Messerly, R. J. Beach, M. Y. Shverdin, A. K. Sridharan, P. H. Pax, J. E. Heebner, C. W. Siders, and C. P. J. Barty, "Ultimate power limits of optical fibers," in *Proc. Opt. Fiber Commun. Conf.*, Mar. 2010, pp. 1–2, Paper OM06.

[28] *Fibercore*. Accessed: Sep. 23, 2019. [Online]. Available: https://www.fibercore.com

[29] Accessed: Sep. 23, 2019. [Online]. Available: http://mathscinotes.com/2017/03/optical-fiber-attenuation-specifications/

[30] B. Zhu, T. F. Taunay, M. F. Yan, J. M. Fini, M. Fishteyn, E. M. Monberg, and F. V. Dimarcello, "Seven-core multicore fiber transmissions for passive optical network," *Opt. Express*, vol. 18, no. 11, pp. 11117–11122, 2010.

[31] K. S. Abedin and T. Morioka, "Remote detection of fiber fuse propagating in optical fibers," in *Proc. Conf. Opt. Fiber Commun.*, San Diego, CA, USA, 2009, pp. 1–3, Paper OthD5.

[32] J. D. López-Cardona, C. Vázquez, D. S. Montero, and P. C. Lallana, "Remote optical powering using fiber optics in hazardous environments," *J. Lightw. Technol.*, vol. 36, no. 3, pp. 748–754, Feb. 1, 2018.

[33] G. Agrawal, *Nonlinear Fiber Optics*. Amsterdam, The Netherlands: Elsevier, 2013.

[34] K. Saitoh and S. Matsuo, "Multicore fiber technology," *J. Lightw. Technol.*, vol. 34, no. 1, pp. 55–66, Jan. 1, 2015.

[35] H. Takara, "1000-km 7-core fiber transmission of 10×96-Gb/s PDM-16QAM using Raman amplification with 6.5 W per fiber," *Opt. Express*, vol. 20, no. 9, pp. 10100–10105, 2012.

[36] K. Takenaga, S. Tanigawa, N. Guan, S. Matsuo, K. Saitoh, and M. Koshiba, "Reduction of crosstalk by quasi-homogeneous solid multi-core fiber," in *Proc. Conf. Opt. Fiber Commun. (OFC/NFOEC)*, San Diego, CA, USA, Mar. 2010, pp. 1–3.

[37] W. Zhi-Yong, Q. Qi, and S. S. Ji, "Temperature dependence of the refractive index of optical fibers," *Chin. Phys. B*, vol. 23, no. 3, 2014, Art. no. 034201.

[38] J. W. Dawson, M. J. Messerly, R. J. Beach, M. Y. Shverdin, E. A. Stappaerts, A. K. Sridharan, P. H. Pax, J. E. Heebner, C. W. Siders, and C. P. J. Barty, "Analysis of the scalability of diffraction-limited fiber lasers and amplifiers to high average power," *Opt. Express*, vol. 16, no. 17, pp. 13240–13266, Aug. 2008.

CARMEN VÁZQUEZ (M'99–SM'05) is currently a Full Professor with the Electronics Technology Department, Universidad Carlos III Madrid (UC3M). She was with TELECOM, Denmark, and Telefonica Investigacion y Desarrollo, Spain. She leads projects, such as SINFOTON2, BlueSPACE, and TEFLON-CM UC3M contributions. She is the Head of Electrical System Applications and Photonics Engineering Master Programmes. Her research interests include integrated optics, optical communications and instrumentation with plastic and multicore optical fibers, fiber optic sensors, power over fiber, and WDM-PON networks. She is a Fellow of SPIE.

JUAN DAYRON LÓPEZ-CARDONA received the M.Sc. degree in electronic systems engineering from the Universidad Carlos III of Madrid (UC3M), Spain, in 2016, where he is currently pursuing the Ph.D. degree in electrical, electronics and automation engineering. His research interests include low power electronics, biomedical applications, multicore optical fibers, and power over fiber systems.

PEDRO CONTRERAS LALLANA received the Ph.D. degree in electrical, electronics and automation engineering from UC3M, in May 2011. His research interests include integrated optics switches, fiber optic sensors, and power-over fiber systems.

DAVID SÁNCHEZ MONTERO received the Ph.D. degree in electrical, electronics and automation engineering from UC3M, in March 2011. Since 2015, he has been a Senior Lecturer with the Electronics Technology Department, UC3M. He is currently involved with the H2020 Bluespace project. His current research interests include fiber-optic sensors, plastic and multicore optical fibers, WDM-PON networks, network monitoring techniques, and power over fiber systems.

FAHAD MOHAMMED ABDULHUSSEIN AL-ZUBAIDI received the M.Sc. degree in laser/electronic and communication engineering from the University of Baghdad, Iraq, in 2015. He is currently pursuing the Ph.D. degree in electrical, electronics and automation engineering with UC3M. His research interests include plastic optical fibers, radio over fiber, and power over fiber systems.

SANDRA PÉREZ-PRIETO received the M.Eng. degree in industrial engineering from the Universidad Carlos III of Madrid (UC3M), Spain, in 2017. She investigated optical fiber sensors designed to measure temperature in the Electrical, Electronics and Automation Engineering Department at UCM3, in 2018.

ISABEL PÉREZ GARCILÓPEZ received the M.Sc. degree in telecommunication engineering from the Polytechnic University of Madrid, in 1995, and the Ph.D. degree from UC3M, in 2003. She is currently an Associate Professor with the Electronics Technology Department, UC3M. She has leaded two national research projects. She is the coauthor of more than 80 articles in JCR journals and contributions to international meetings. Her research interests include electrooptical characterization and modeling of liquid crystal (LC) cells, LC and fiber optics devices, and the development of new applications.